

Experimental and computational study of the conrotatory ring opening of various 3-chloro-2-azetines

Sven Mangelinckx,^a Veronique Van Speybroeck,^b Peter Vansteenkiste,^b Michel Waroquier,^b
Norbert De Kimpe^{a,*}

^aDepartment of Organic Chemistry, Faculty of Bioscience Engineering, Ghent University, Coupure Links 653, B-9000 Ghent, Belgium; ^bCenter of Molecular Modeling, Ghent University, Proeftuinstraat 86, B-9000 Ghent, Belgium

Contents:

General information and spectroscopic data for compounds 12b/13b and 12c/13c	S2
Computational details	S4
¹ H and ¹³ C NMR spectra of new compounds	S8

General Information

^1H NMR spectra (300 MHz) and ^{13}C NMR spectra (75 MHz) were recorded with CDCl_3 or $\text{DMSO}-d_6$ as solvent and tetramethylsilane (TMS) as internal standard. For liquid samples, the IR spectra were recorded by preparing a thin film of compound between sodium chloride plates. Solid compounds were mixed with potassium bromide and pressed at high pressure until a transparent disc was obtained. Mass spectra were recorded using a direct inlet system (ES, 4000V) *via* LC-MS. Melting points of crystalline compounds are not corrected. Column chromatography was performed with silica gel (particle size 0.035–0.070 mm, pore diameter ca. 6 nm) using a glass column. Tetrahydrofuran was distilled over sodium benzophenone ketyl, DMSO was distilled and kept over molecular sieves. Methanol was dried with magnesium and distilled, while other solvents were used as received from the supplier. Commercially available reagents were purchased from common chemical suppliers and used without further purification.

***N*-[3-(4-methylphenyl)-1-phenylprop-2-yn-1-ylidene]propyl-2-amine 12b and *N*-[1-(4-methylphenyl)-3-phenylprop-2-yn-1-ylidene]propyl-2-amine 13b.** Spectral data obtained from the mixture of **12b/13b** in a ratio 2/1. Underlined data are from **13b**. ^1H NMR (CDCl_3 , 300 MHz): δ = 1.305 (d, 3H, J = 6.33 Hz), 1.310 (d, 6H, J = 6.33 Hz), 2.39 (s, 1.5H), 2.40 (s, 3H), 4.32 (septet, 0.5H, J = 6.33 Hz), 4.33 (septet, 1H, J = 6.33 Hz), 7.19–7.23, 7.36–7.50, 7.55–7.60, 7.94–7.98, 8.04–8.09 (m, 13.5H); ^{13}C NMR (CDCl_3 , 75 MHz): δ = 21.4, 21.6, 23.5, 56.19, 56.22, 81.1, 81.7, 97.2, 97.9, 118.7, 121.8, 127.47, 127.53, 128.2, 128.5, 128.9, 129.3, 129.5, 130.1, 132.05, 132.07, 135.3, 138.0, 139.9, 140.4, 148.2, 148.5; IR (NaCl, cm^{-1}): ν = 2203 ($\text{C}\equiv\text{C}$), 1591 ($\text{C}=\text{N}$); MS (ES, pos. mode): m/z (%): 262 ($\text{M}+\text{H}^+$, 100). Anal. Calcd for $\text{C}_{19}\text{H}_{19}\text{N}$: C 87.31; H 7.33; N 5.36. Found: C 87.05; H 7.28; N 5.29. Yield = 84%. R_f = 0.18 (petroleum ether/EtOAc 96/4). Colorless viscous oil.

***N*-[3-(4-chlorophenyl)-1-phenylprop-2-yn-1-ylidene]propyl-2-amine 12c and *N*-[1-(4-chlorophenyl)-3-phenylprop-2-yn-1-ylidene]propyl-2-amine 13c.** Spectral data obtained from the mixture of **12c/13c** in a ratio 1/2.3. Underlined data are from **12c**. ¹H NMR (CDCl₃, 300 MHz): δ = 1.30 (d, 6H, *J* = 6.05 Hz), 1.31 (d, 2.6H, *J* = 6.33 Hz), 4.30 (septet, 0.43H, *J* = 6.33 Hz), 4.31 (septet, 1H, *J* = 6.33 Hz), 7.35-7.61, 7.99-8.07 (m, 12.9H); ¹³C NMR (CDCl₃, 75 MHz): δ = 23.50, 23.54, 56.4, 81.1, 82.3, 96.1, 97.8, 120.1, 121.5, 127.5, 128.3, 128.4, 128.6, 128.8, 128.9, 129.7, 130.3, 132.1, 133.3, 135.7, 136.2, 136.3, 137.7, 147.1, 148.0; IR (NaCl, cm⁻¹): ν = 2205 (C \equiv C), 1587 (C=N); MS (ES, pos. mode): *m/z* (%): 282/84 (M+H⁺, 100). Anal. Calcd for C₁₈H₁₆ClN: C 76.72; H 5.72; N 4.97. Found: C 76.54; H 5.75; N 4.86. Yield = 79%. R_f = 0.21 and 0.12 (petroleum ether/EtOAc 97/3). Light yellow viscous oil.

Computational details

All ab initio calculations were performed with Gaussian03¹ at the mPW1B95/6-31+G(d,p)² level of theory. This level is expected to be a reliable method for reproducing accurate geometries and energy values of molecules with heteroelements³ in general. More particularly, it was found to be the most appropriate level to describe simple four-membered rings⁴. These papers do not deal with the considered type of reactions, but in a recent paper, it was established that the conrotatory ring opening of bicyclobutane to 1,3-butadiene is well described by the general purpose B3LYP DFT functional⁵. This fact reinforces our choice for DFT. In order to obtain the correct reaction mechanism of conrotatory ring opening of the C4-N1 bond, first the geometry of each (substituted) 2-azetidine is optimized. For compounds **28**, **3**, **29**, **30**, **14aT**, **14aC**, with the isopropyl substitution at nitrogen, there are several conformations (rotamers) possible. These conformers are found by calculating the relaxed potential energy scan of the internal rotation of the isopropyl substituent, and fully optimizing the local minima. Starting from each such optimized geometry, another relaxed potential

¹ Gaussian 03, Revision B.03 and Revision D.01, Frisch, M. J.; Trucks, G. W.; Schlegel, H. B.; Scuseria, G. E.; Robb, M. A.; Cheeseman, J. R.; Montgomery, Jr., J. A.; Vreven, T.; Kudin, K. N.; Burant, J. C.; Millam, J. M.; Iyengar, S. S.; Tomasi, J.; Barone, V.; Mennucci, B.; Cossi, M.; Scalmani, G.; Rega, N.; Petersson, G. A.; Nakatsuji, H.; Hada, M.; Ehara, M.; Toyota, K.; Fukuda, R.; Hasegawa, J.; Ishida, M.; Nakajima, T.; Honda, Y.; Kitao, O.; Nakai, H.; Klene, M.; Li, X.; Knox, J. E.; Hratchian, H. P.; Cross, J. B.; Adamo, C.; Jaramillo, J.; Gomperts, R.; Stratmann, R. E.; Yazyev, O.; Austin, A. J.; Cammi, R.; Pomelli, C.; Ochterski, J. W.; Ayala, P. Y.; Morokuma, K.; Voth, G. A.; Salvador, P.; Dannenberg, J. J.; Zakrzewski, V. G.; Dapprich, S.; Daniels, A. D.; Strain, M. C.; Farkas, O.; Malick, D. K.; Rabuck, A. D.; Raghavachari, K.; Foresman, J. B.; Ortiz, J. V.; Cui, Q.; Baboul, A. G.; Clifford, S.; Cioslowski, J.; Stefanov, B. B.; Liu, G.; Liashenko, A.; Piskorz, P.; Komaromi, I.; Martin, R. L.; Fox, D. J.; Keith, T.; Al-Laham, M. A.; Peng, C. Y.; Nanayakkara, A.; Challacombe, M.; Gill, P. M. W.; Johnson, B.; Chen, W.; Wong, M. W.; Gonzalez, C. and Pople, J. A.; Gaussian, Inc., Pittsburgh PA,

² (a) Zhao, Y.; Truhlar, D. G. *J. Phys. Chem. A*, **2004**, *108*, 6908. (b) Hehre, W. J.; Radom, L.; Schleyer, P. v. R.; Pople, J. A. *Ab Initio Molecular Orbital Theory* Wiley: New York, **1986**.

³ (a) Zhao, Y.; Truhlar, D. G. *J. Phys. Chem. A*, **2005**, *109*, 5656. (b) Zheng, J.; Zhao, Y.; Truhlar, D. G. *J. Chem. Theory Comput.*, **2007**, *3*, 569.

⁴ Vansteenkiste, P.; Van Speybroeck, V.; Verniest, G.; De Kimpe, N.; Waroquier, M. *J. Phys. Chem. A*, **2006**, *110*, 3838. (b) Vansteenkiste, P.; Van Speybroeck, V.; Verniest, G.; De Kimpe, N.; Waroquier, M. *J. Phys. Chem. A*, **2007**, *111*, 2797.

⁵ Kinal, A. and Piecuch P., *J. Phys. Chem. A*, **2007**, *111*, 734.

energy scan is calculated, now as a function of the C4--N1 length. This results in ten energy data points for the structures with the C4---N1 distance varying from 1.6 Å to a length of 2.5 Å with increments of 0.1 Å. Since the increments are rather small, this kind of calculation is expected to provide the preferred reaction path of the ring opening. The transition states were further optimized using the option TS in Gaussian with an additional frequency calculation to verify the true nature of the transition states. Furthermore for representative reactions of each class, the transition states were verified by using the option QST3 in Gaussian.

In addition, the structures of the products are fully optimized. Also the transition states are calculated, and verified to be single order saddle points by a frequency calculation. The investigation of the C4-N1 ring opening reaction of each starting structure involves the calculation of at least 13 energy data. As an example, the data of the ring opening reaction of 2,4-diphenyl-3-chloro-2-azetine **20** are displayed in Figure S.1. The 3D structures shown are all fully optimized. It illustrates the differences of the inwards and outwards conrotatory mechanism very well. Note that all reported energy values are without the inclusion of zero point energy.

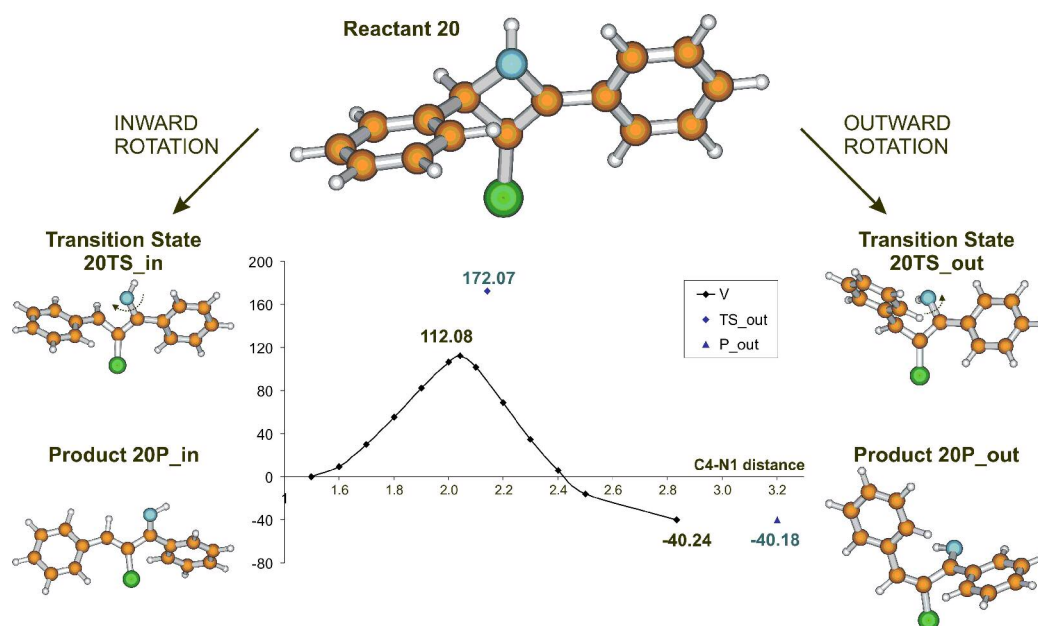


Figure S.1 : Example of typical data obtained for each calculation of the ring opening reaction. The solid line includes the relaxed potential energy scan, and the energies of the optimized starting geometry (reactant), of the optimized transition state, and of the optimized product. In this case, for compound **20**, the scan results in the inward conrotatory ring opening. The isolated points are the energies of the optimized transition state and product of the opposite, in this case outward, conrotatory mechanism.

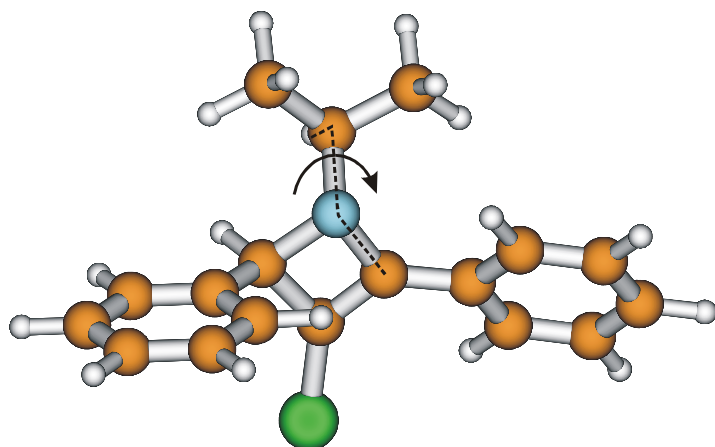


Figure S.2 : Compound **14aT** in most favored energy conformation.

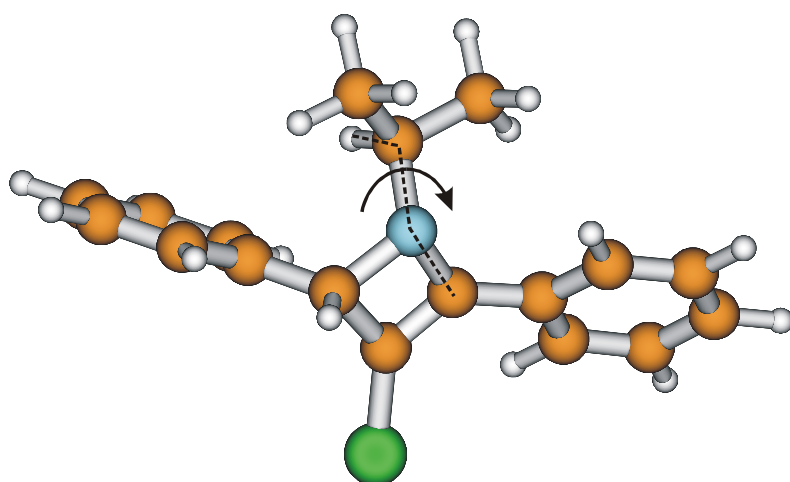


Figure S.3 : Compound **14aC** in most favored energy conformation.

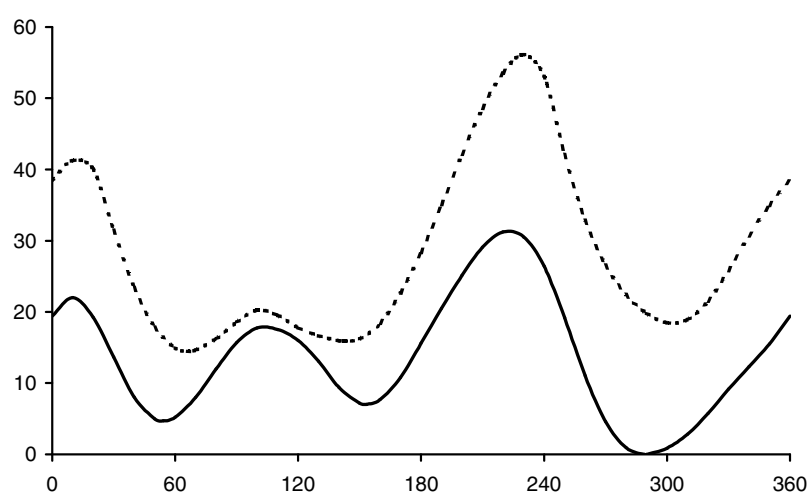


Figure S.4 : Isopropyl rotational profiles for the compounds **14aT** (full line) and **14aC** (dashed line).

^1H and ^{13}C NMR spectra of new compounds

